*Organometallics* **1992,** *11,* 3691–3696

# Structure and Bonding in Group 4 Metallocene Acetylide and Metallacyclopentadiene Complexes

Eugene T. Knight, Lori K. Myers, and Mark E. Thompson*

*Department of Chemistry, Princeton University, Princeton, New Jersey 08544*

*Received May 19, 1992*

Ab initio methods (STO-3G basis set) have been used to obtain structures for $Cp_2Ti(C{\equiv}CR)_2$ (R = Me, H) and $Cp_2\overline{TiCH{=}CHCH{=}C}H$. Both ab initio (3-21G and 6-31G basis sets) and semiempirical (ZINDO) calculations were carried out on the optimized structures to examine the energies and atomic orbital compositions of the complexes' molecular orbitals. Evidence for extensive mixing between alkynyl $\pi$ and "$Cp_2Ti$" bonding orbitals is seen in these calculations. The proposed mechanism for this mixing involves interactions between filled acetylide $\pi$ and Cp–Ti bonding orbitals. Very little evidence is seen for $\pi$ donation from filled acetylide orbitals to vacant metal-based orbitals. In addition very little mixing is observed between the ligand $\pi$ orbitals and the Cp–Ti bonding orbitals of ($Cp_2\overline{TiCH{=}CHCH{=}C}H$). The lack of mixing in both of these situations arises from poor energy matching of the interacting orbitals, since the degree of orbital overlap in both cases is similar to that observed for $Cp_2Ti(C{\equiv}CR)_2$.

## Introduction

Tetravalent group 4 metallocenes ($Cp_2MX_2$) have been extensively studied[1] since their initial report in the early 1950s.[2] These complexes have a pseudotetrahedral geometry, with the cyclopentadienyl ligands occupying two sites and the remaining two ligands lying in the wedge formed by the Cp rings (Figures 1 and 2). A great deal of the reactivity of these complexes comes from their high Lewis acidity and coordinate unsaturation (formally $M^{IV}$, 16-electron complexes). Group 4 metallocenes are very active at both stoichiometric and catalytic transformations of organic substrates.[1,3] High molecular weight polymers can be prepared with metallocene-based catalysts.[1,4] The use of these complexes to prepare inorganic polymers has also been reported recently.[5]

We have been studying the third-order nonlinear optical (NLO) properties of group 4 metallocenes. The measured NLO coefficients, $\gamma$, of $Cp_2M(C{\equiv}CC_6H_5)_2$ (for M = Ti, Zr, and Hf, $\gamma$ ($\times 10^{36}$) = 90, 60, and 50 esu, respectively) are all greater than their organic analogs.[6] Materials with large nonresonant third-order NLO susceptibilities typically have delocalized $\pi$ systems.[7,8] The NLO properties of group 4 metallocene acetylides clearly come from a delocalized electronic system involving the metal orbitals. The theoretical calculations reported herein are aimed at identifying the nature of this delocalized system.

Tetravalent group 4 metallocenes have been studied theoretically using various levels of sophisitication. Most of the calculations have focused on the halide, hydride, and alkyl complexes, due to their importance in synthetic chemistry. Both Fenske–Hall and extended Hückel approaches have been used to assign electronic spectra and to understand the structure and bonding in these complexes.[9] More exact SCF-X$\alpha$-SW calculations have been used to accurately assign both electronic and photoelectron spectra of the metallocene dihalide complexes.[10] The picture that emerges from these calculations and spectroscopic studies[9e] of three of the dihalides ($Cp_2TiX_2$; X = F, Cl, Br) is that the higher energy occupied orbitals (HOMOs) are Cp–metal bonding in character and the LUMO is a metal-localized orbital (Figure 2) lying in the wedge of the metallocene molecule. Similar studies carried out on the diiodo- and dimethyltitanocene complexes indicate that the HOMOs have a reasonable amount of iodine p and Ti–$CH_3$ $\sigma$-bonding character, respectively, while the LUMO is thought to be the same as for the other halides. Recently ab initio calculations have been carried out on $Cp_2TiX_2$ complexes.[11] The goals of these studies

---

(1) See: (a) Wailes, P. C.; Coutts, R. S. P.; Wegold, H. *Organometallic Chemistry of Titanium, Zirconium and Hafnium*; Academic Press: New York, 1974. (b) Thewalt, U. *Gmelin Handbook of Inorganic Chemistry*; Slawisch, A., Ed.; Springer Verlag: Berlin, 1984; 8th edition, Part 4. (c) Cardin, D. J.; Lappert, M. F.; Raston, C. L. *Chemistry of Organo-Zirconium and -Hafnium Compounds*; John Wiley & Sons: New York, 1986.

(2) (a) Ethyl Corp. Ger. Pat. 1 217 952, 1966; *Chem. Abstr.* **1964,** *61,* 5434. (b) Wilkinson, G.; Pauson, P. L.; Birmingham, J. M.; Cotton, F. A. *J. Am. Chem. Soc.* **1953,** *75,* 1011. (c) Wilkinson, G.; Birmingham, J. M. *J. Am. Chem. Soc.* **1954,** *76,* 4281.

(3) For example see: (a) Schwartz, J. *Pure Appl. Chem.* **1980,** *52,* 733. (b) Negishi, E. *Pure Appl. Chem.* **1981,** *53,* 2333. (c) Erker, G.; Engel, K.; Atwood, J. L.; Hunter, N. E. *Angew. Chem., Int. Ed. Engl.* **1983,** *22,* 494. (d) Brown-Wensley, K. A.; Buchwald, S. L.; Canizzo, L.; Clawson, L.; Ho, S.; Meinhardt, D.; Stille, J. R.; Straus, D.; Grubbs, R. H. *Pure Appl. Chem.* **1983,** *55,* 1733. (e) Buchwald, S. L.; Nielsen, R. B. *Chem. Rev.* **1988,** *88,* 1047.

(4) (a) Sinn, H.; Kaminsky, W. *Adv. Organomet. Chem.* **1980,** *18,* 99. (b) Reichert, K. H. *Transition Metal Catalyzed Polymerizations. Alkenes and Dienes*; Quirk, R. P., Ed.; Harwood Academic: New York, 1983; Part B, p 465. (c) Kaminsky, W.; Spiehl, R. *Macrnol. Chem.* **1989,** *190,* 515. (d) Jordan, R. F.; Najgur, C. S.; Willett, R.; Scott, B. *J. Am. Chem. Soc.* **1986,** *108,* 7410. (e) Hlatky, G. G.; Turner, H. W.; Eckman, R. R. *J. Am. Chem. Soc.* **1989,** *111,* 2728.

(5) (a) Tilley, T. D. *Comments Inorg. Chem.* **1990,** *10,* 37. (b) Harrod, J. F.; Yun, S. S. *Organometallics* **1987,** *6,* 1381.

(6) Myers, L. K.; Thompson, M. E.; Langhoff, C. *J. Am. Chem. Soc.* **1992,** *114,* 7560.

(7) (a) Prasad, P. N.; Williams, D. J. *Nonlinear Optical Effects in Molecules and Polymers*; John Wiley and Sons, Inc.: New York, 1991. (b) Ulrich, D. R. *Mol. Cryst. Liq. Cryst.* **1990,** *189,* 3. (c) Chemla, D. S.; Zyss, T. *Nonlinear Optical Properties of Organic Molecules and Crystals*; Academic Press, Inc.: Orlando, FL, 1987; Vol. 2.

(8) (a) Frazier, C. C.; Guha, S.; Chen, W. P.; Cockerham, M. P.; Porter, P. L.; Chauchard, E. A.; Lee, C. H. *Polymer* **1987,** *28,* 553. (b) Cheng, L.-T.; Tam, W.; Meredith, G. R.; Marder, S. R. *Mol. Cryst. Liq. Cryst.* **1990,** *189,* 137. (c) For a recent review, see: Nalwa, H. S. *Appl. Organomet. Chem.* **1991,** *5,* 349.

(9) (a) Green, J. C.; Green, M. L. H.; Prout, C. K. *J. Chem. Soc., Chem. Commun.* **1972,** 421. (b) Petersen, J. L.; Lichtenberger, D. L.; Fenske, R. F.; Dahl, L. F. *J. Am. Chem. Soc.* **1975,** *97,* 6422. (c) Petersen, J. L.; Dahl, L. F. *J. Am. Chem. Soc.* **1975,** *97,* 6433. (d) Lauher, J. W.; Hoffmann, R. *J. Am. Chem. Soc.* **1976,** *98,* 1729. (e) Cauletti, C.; Clark, J. P.; Green, J. C.; Fragala, I. L.; Ciliberto, E.; Coleman, A. W. *J. Electron Spectrosc. Relat. Phenom.* **1980,** *18,* 61.

(10) Bruce, M. R. M.; Kenter, A.; Tyler, D. R. *J. Am. Chem. Soc.* **1984,** *106,* 639.

(11) (a) Jolly, C. A.; Marynick, D. S. *J. Am. Chem. Soc.* **1989,** *111,* 7968. (b) Francl, M. M.; Pietro, W. J.; Hout, R. F.; Hehre, W. J. *Organometallics* **1983,** *2,* 281. (c) Francl, M. M.; Pietro, W. J.; Hout, R. F.; Hehre, W. J. *Organometallics* **1983,** *2,* 815. (d) Hansen, L. M.; Marynick, D. S. *Organometallics* **1989,** *8,* 2173.

0276-7333/92/2311-3691\$03.00/0

**Table I. Bond Lengths and Angles for $\mathrm{Cp_2Ti(C{\equiv}CR)_2}$ (R = Me, H) and $\mathrm{Cp_2\overline{TiCR'{=}CR'CR'{=}C}R'}$ (R′ = H, Ph)**

| | $\mathrm{Cp_2Ti(C{\equiv}CMe)_2}$ | $\mathrm{Cp_2Ti(C{\equiv}CH)_2}$ | $\mathrm{Cp_2\overline{TiCH{=}CHCH{=}C}H}$ | $\mathrm{Cp_2\overline{TiCPh{=}CPhC{=}C}Ph}^a$ |
|---|---|---|---|---|
| | | Distances (Å)$^c$ | | |
| Ti–C(Cp), av | 2.356 | 2.352 | 2.356 | 2.386 (22) |
| Ti–$C_\alpha$ | 2.071 | 2.077 | 2.111 | 2.155 (5) |
| $C_\alpha$–$C_\beta$ | 1.183 | 1.181 | 1.321 | 1.370 (6) |
| $C_\beta$–R | 1.483 | 1.063 | 1.086 | |
| $C_\beta$–$C_{\beta'}$ | | | 1.496 | 1.495 (6) |
| $C_1$–$C_2$ | 1.411 | 1.412 | 1.411 | |
| $C_2$–$C_3$ | 1.408 | 1.409 | 1.409 | |
| $C_3$–$C_{3'}$ | 1.423 | 1.423 | 1.423 | |
| | | Angles (deg)$^c$ | | |
| $C_\alpha$–Ti–$C_\alpha$ | 93.0 | 92.6 | 80.9 | 80.3 (2) |
| Ti–$C_\alpha$–$C_\beta$ | $180^b$ | $180^b$ | 111.4 | 111.0 (3) |
| $C_\alpha$–$C_\beta$–R | $180^b$ | $180^b$ | 124.0 | 123.5 (3) |
| $C_\alpha$–$C_\beta$–$C_{\beta'}$ | | | 118.1 | 118.0 (4) |
| centroid–Ti–centroid | 136 | 136 | 136 | 134.8 (3) |

[a] Ph = $C_6H_5$. Atwood, J. L.; Hunter, W. E.; Alt, H.; Rausch, M. D. *J. Am. Chem. Soc.* **1976**, *98*, 2454. [b] These angles were held fixed at 180°. [c] $C_1$, $C_2$, and $C_3$ are the Cp carbons, with $C_1$ lying in the *yz* plane. $C_\alpha$ and $C_\beta$ are the carbons of the propyde and metallacycle ligands. R is the methyl carbon for $\mathrm{Cp_2Ti(C{\equiv}CMe)_2}$, the acetylide proton for $\mathrm{Cp_2Ti(C{\equiv}CH)_2}$, and the proton bound to the $\beta$ carbon of the metallacycle for $\mathrm{Cp_2\overline{TiCH{=}CHCH{=}C}H}$.

**Figure 1.** $\mathrm{Cp_2Ti(C{\equiv}CR)_2}$ (left) and $\mathrm{Cp_2\overline{TiCH{=}CHCH{=}C}H}$ (right).

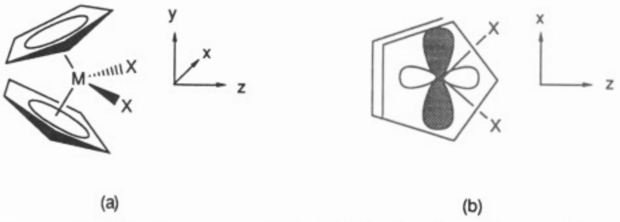

**Figure 2.** (a) Structure of $\mathrm{Cp_2MX_2}$, showing the coordinate system used in this study. (b) Proposed LUMO for $\mathrm{Cp_2MX_2}$ compounds, M = Ti, Zr, and Hf.

involve the examination of equilibrium structures and conformational preferences for the molecules. The energies of the molecular orbitals generated by ab initio methods typically deviate further from the experimentally determined values than those obtained from semiempirical methods. However, ab initio methods generally give structures much closer to experimentally observed ones and are expected to give a more accurate picture of the atomic compositions of the molecular orbitals than semiempirical calculations.[12] A common substitution made in these more detailed calculations is to approximate the Cp as a chloride or hydride ligand. While this simplication saves a great deal of time computationally,[13] it may lead to a misleading picture of the electronic structure in the complex of interest.[11] For this reason we chose to use the full $C_5H_5$ ligand in our calculation.

No theoretical studies have been reported for group 4 metallocenes with either $\sigma$-bound alkynyl or vinylic ligands.

**Table II. Orbital Compositions for the LUMO and the Top Eight Filled Molecular Orbitals of $\mathrm{Cp_2Ti(C{\equiv}CR)_2}$**

| | | Ti:alkyne:Cp$^b$ | | |
|---|---|---|---|---|
| orbital | energy (eV)$^a$ | R = H, STO-6-31G | R = H, STO-3G | R = Me, STO-3G$^c$ |
| LUMO-$23a_1$ | | 56:22:22 | 59:16:25 | 58:16:26 |
| HOMO-$14b_1$ | −7.7 | 8:31:61 | 5:43:52 | 3:50:46 |
| $7a_2$ | −8.0 | 9:49:42 | 4:63:33 | 2:67:30 |
| $16b_2$ | −8.9 | 3:59:38 | 1:84:15 | 1:84:14 |
| $22a_1$ | −9.4 | 17:13:70 | 17:8:75 | 18:6:74 |
| $15b_2$ | −9.6 | 12:40:48 | 18:23:59 | 19:18:63 |
| $13b_1$ | −10.2 | 10:66:24 | 10:54:36 | 11:42:46 |
| $21a_1$ | −10.7 | 7:81:12 | 4:92:4 | 4:88:8 |
| $6a_2$ | −11.1 | 15:50:35 | 13:36:51 | 14:27:58 |

[a] Energies calculated for $\mathrm{Cp_2Ti(C{\equiv}CH)_2}$ by ZINDO. [b] Ratio of Ti:alkyne:Cp atomic orbitals in the given molecular orbital. [c] Ratios which do not sum to 100% have the remainder composed of Me C orbitals.

We have used ab initio methods (STO-3G basis set) to obtain structures for $\mathrm{Cp_2Ti(C{\equiv}CR)_2}$ (R = Me, H) and $\mathrm{Cp_2\overline{TiCH{=}CHCH{=}C}H}$ (Figure 1). Ab initio (3-21G and 6-31G basis sets) and semiempirical (ZINDO) calculations were carried out on the optimized structures to examine the energies and atomic orbital compositions of the complexes' molecular orbitals. For the compounds reported herein we had a number of questions concerning their electronic structure. What would the nature of the HOMOs be? Will the HOMOs of these complexes be Ti–C $\sigma$ bonding (as in $\mathrm{Cp_2TiMe_2}$) or Cp-M $\pi$ bonding (as in $\mathrm{Cp_2TiX_2}$, X = F, Cl, Br)? Will there by any interaction between the filled $\pi$ orbitals of the acetylide or metallocycle ligands and the vacant metal orbitals?

## Results

Since crystallographic data were not available for any of the complexes which we felt were accessible by ab initio calculations, the first step was to determine the minimum energy structures. The metallocene Cp rings were forced to stay eclipsed throughout the geometry minimization. This conformation of Cp rings and choice of coordinate system are shown in Figure 2. The eclipsed conformation of Cp ligands gives the complex the highest symmetry ($C_{2v}$). Both eclipsed and staggered ring conformations have been observed in group 4 bent metallocenes, and the barrier to their interconvesion is negligible.[14] The geom-

---

[12] Hehre, W. J.; Radom, L.; Schleyer, P. vR.; Pople, J. A. *Ab Initio Molecular Orbital Theory*; John Wiley & Sons: New York, 1986.

[13] (a) Fujimoto, H.; Yamasaki, T.; Mizutani, H.; Koga, N. *J. Am. Chem. Soc.* **1985**, *107*, 6157. (b) Navaro, O.; Blaisten-Barojas, E.; Clementi, E.; Giunchi, G.; Ruiz-Vicaya, M. E. *J. Chem. Phys.* **1978**, *68*, 2337. (c) Steigerwald, M. L.; Goddard, W. A. III. *J. Am. Chem. Soc.* **1985**, *107*, 5027. (d) Steigerwald, M. L.; Goddard, W. A., III. *J. Am. Chem. Soc.* **1984**, *106*, 308. (e) Rappe, A. K. *J. Am. Chem. Soc.* **1987**, *109*, 5605. (f) Bursten, B. E. *Pure Appl. Chem.* **1991**, *63*, 839.

**Table III. Breakdowns of the Atomic Orbital Contributions from Individual Alkynyl and Cp Carbons to the LUMO and Top Eight Filled MOs of $Cp_2Ti(C{\equiv}CH)_2$ with the Calculation Carried out at the 6-31G Level**

| | % alkyne[a] | | % Cp[a] | | | |
|---|---|---|---|---|---|---|
| orbital | $\alpha$ | $\beta$ | 1 | 2 | 3 | Ti:alkyne:Cp |
| LUMO-23$a_1$ | 4 | 18 | 10 | 10 | 2 | 56:22:22 |
| HOMO-14$b_1$ | 10 | 21 | 29 | 6 | 26 | 8:31:61 |
| 7$a_2$ | 19 | 30 | 3 | 28 | 14 | 9:49:42 |
| 16$b_2$ | 25 | 34 | 0 | 22 | 15 | 3:59:38 |
| 22$a_1$ | 7 | 5 | 32 | 8 | 30 | 17:13:70 |
| 15$b_2$ | 21 | 20 | 0 | 31 | 17 | 12:40:48 |
| 13$b_1$ | 32 | 33 | 6 | 1 | 17 | 10:66:24 |
| 21$a_1$ | 43 | 39 | 2 | 2 | 8 | 7:81:12 |
| 6$a_2$ | 25 | 25 | 4 | 27 | 8 | 15:50:35 |

[a] Numbering of alkynyl and Cp carbons is the same as that used in Table I.

etry optimization was carried out by ab initio methods at the STO-3G basis set level.[15] The bond lengths and angles for the minimized structures are given in Table I. The optimized angles and bond lengths are well within the ranges observed for other $Cp_2TiX_2$ complexes.[1] For comparison, the analogous bond lengths and angles from the crystal structure of $Cp_2\overline{\text{TiCPh=CPhCPh=C}}\text{Ph}$ are also given in Table I.

The orbital compositions obtained for the LUMO and the top eight filled MOs for $Cp_2Ti(C{\equiv}CR)_2$ (R = Me, H) are given in Table II. The energies listed in the table are estimated using a semiempirical calculation, based on the optimized structure for $Cp_2Ti(C{\equiv}CH)_2$. The semiempirical calculation was carried out using the INDO/S electronic structure formalism developed by Zerner (ZINDO) with a configuration interaction level of 10 (10 HOMOs and 10 LUMOs).[16] To have faith in the results of these ab initio calculations, it is important to carry them out with the most complete basis set possible. With the available computing facilities it was not feasible to optimize the geometry at a level higher than 3G. For this reason the geometry determined at 3G was used for single point calculations, carried out using split valence basis sets (3-21G and 6-31G). To minimize the computational time required at the higher basis sets, $Cp_2Ti(C{\equiv}CH)_2$ was used rather than $Cp_2Ti(C{\equiv}CMe)_2$. The orbital compositions obtained from the 3-21G and 6-31G calculations were very similar, and only the 6-31G data will be discussed (6-31G data given in Table II). The orbital compositions obtained from the 6-31G calculations for the top eight filled valence orbitals and the LUMO are listed in Table II. Breakdowns of the contributions from individual alkynyl and Cp carbons to these orbitals are given in Table III. It should be noted that the Ti–C $\sigma$-bonding orbitals are not listed in Tables II or III; they are the ninth and tenth filled valence orbitals for $Cp_2Ti(C{\equiv}CR)_2$ (14$b_2$ and 20$a_1$, −12.5 and −12.8 eV, respectively).[17]

The HOMO (14$b_1$) has contributions from alkynyl, Cp, and metal orbitals, regardless of which basis set is used. The orbital is composed of roughly 30% alkynyl $\pi$ orbitals, with the remaining 70% made up of Cp $\pi$ and metal d orbitals (6-31G level). Molecular orbital plots of the HOMO are shown in Figure 3.[18] The SHOMO orbital (7$a_2$) has even more mixing between the alkyne $\pi$ and Cp orbitals than the HOMO. To further investigate the degree of mixing between alkyne and Cp orbitals in the HOMO, a single-point UHF calculation was carried out on $Cp_2Ti(C{\equiv}CH)_2^+$ (3G level). The advantage this has over neutral $Cp_2Ti(C{\equiv}CH)_2$ is that it will better account for electron correlation effects. The ratio of Ti:alkyne:Cp atomic orbitals in the highest filled $b_1$ orbital of the cation radical (HOMO in the neutral compound) is 1:63:36. While the ratio of alkyne to Cp orbital population has changed in favor of the alkyne relative to the neutral complex (5:43:52 for neutral at 3G level), the HOMO still shows a high degree of mixing between alkyne $\pi$ and Cp orbitals.

The LUMO orbital for $Cp_2Ti(C{\equiv}CR)_2$ is an $a_1$ symmetry MO, which is predominantly composed of metal orbitals (59%). Molecular orbital plots of the LUMO are shown in Figure 3. The composition and shape of this

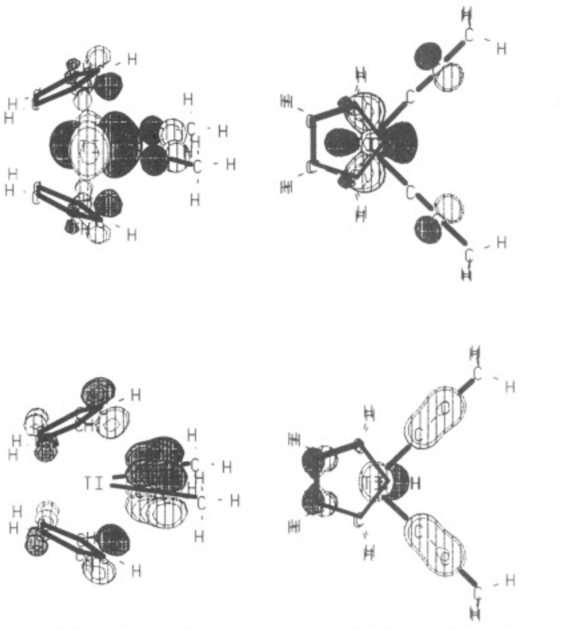

**Figure 3.** Molecular orbital plots[18] for the LUMO and HOMO of $Cp_2Ti(C{\equiv}CMe)_2$: LUMO-23$a_1$ (top) and HOMO-14$b_1$ (bottom). The view to the left is ca. along the $x$ axis, and the view to the right is along the $y$ axis.

**Table IV. Orbital Compositions for the LUMO and the Top Eight Filled Molecular Orbitals of $Cp_2\overline{\text{TiCH=CHCH=C}}\text{H}$ with the Calculation Carried out at the 3G Level**

| orbital | energy (eV)[a] | $Ti:C_4H_4$: $Cp$[b] | orbital type |
|---|---|---|---|
| LUMO-21$a_1$ | | 61:3:36 | Cp–M bonding |
| HOMO-6$a_2$ | −6.6 | 0:91:9 | $C_4H_4$ $\pi$ bonding |
| 12$b_1$ | −7.9 | 8:20:72 | Cp–M + $C_4H_4$ $\pi$ bonding |
| 20$a_1$ | −8.8 | 25:60:15 | Ti–$C_4H_4$ $\sigma$ bonding |
| 12$b_2$ | −9.2 | 26:44:30 | Cp–M $\pi$ + Ti–$C_4H_4$ $\sigma$ bonding |
| 5$a_2$ | −10.2 | 16:8:76 | Cp–M $\pi$ bonding |
| 19$a_1$ | −10.3 | 16:14:70 | Cp–M $\pi$ bonding |
| 11$b_2$ | −10.5 | 19:26:55 | Cp–M $\pi$ + Ti–$C_4H_4$ $\sigma$ bonding |
| 11$b_1$ | −11.1 | 6:77:17 | $C_4H_4$ $\pi$ bonding |

[a] The orbital energies given are based on a ZINDO calculation. [b] Ratio of Ti:alkyne:Cp atomic orbitals in the given molecular orbital.

---

[14] Prout, K.; Cameron, T. S.; Forder, R. A.; Critchley, S. R.; Denton, B. R.; Rees, G. V. *Acta. Crystallogr., Sect. B* **1974**, *30*, 2290.

[15] Special care was required to obtain the electronic ground state. The default methods generated a stable, excited state. The initial guess was altered by the usual methods to produce the ground state.

[16] (a) Anderson, W. P.; Edwards, W. D.; Zerner, M. C. *Inorg. Chem.* **1986**, *25*, 2728. (b) Anderson, W. P.; Cundari, T. R.; Drago, R. S.; Zerner, M. C. *Inorg. Chem.* **1990**, *29*, 1. (c) Kotzian, M.; Rösch, N.; Schröder, H.; Zerner, M. C. *J. Am. Chem. Soc.* **1989**, *111*, 7687 and references therein.

[17] The $a_1$ and $b_2$ symmetry Ti–C $\sigma$-bonding orbitals of $Cp_2Ti(C{\equiv}CR)_2$ are formed as described in ref 7d,e.

[18] The general shape of the STO-3G orbitals are the same as those from the split valance basis sets (3-21G and 6-31G). The MO plots for the split valence orbitals would have the same shape, sign, and disposition for the lobes as seen in the 3G drawings, but the sizes of the lobes would be different.

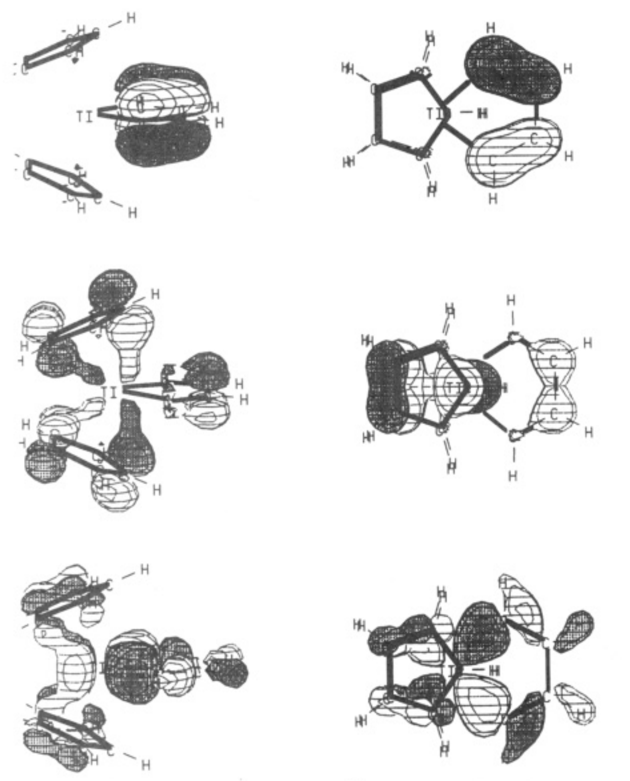

**Figure 4.** Molecular orbital plots[18] of selected MOs of $Cp_2\overline{TiCH{=}CHCH{=}C}H$: HOMO-$6a_2$ (top), SHOMO-$12b_1$ (middle), and $12b_2$ (bottom). The view to the left is ca. along the $x$ axis, and the view to the right is along the $y$ axis.

orbital is similar to that found for the LUMO in calculations on other $Cp_2MX_2$ complexes.[9d,10] To get a better picture of the LUMO orbital in this complex, a single-point calculation was carried out on $Cp_2Ti(C{\equiv}CH)_2^-$. Populating the LUMO gives a much more reliable estimate for its orbital composition, because of the inclusion of both electron–electron repulsion and electron correlation in the calculation for this orbital. The ratio of Ti:alkyne:Cp atomic orbitals in the HOMO of this radical anion (LUMO in the neutral complex) is 72:15:13, showing the predominance of metal character.

The orbital compositions for the LUMO and top eight filled orbitals for $Cp_2\overline{TiCH{=}CHCH{=}C}H$ are given in Table IV. The energies given are taken from a semiempirical calculation (ZINDO) carried out on the optimized geometry with a CI level of 10 (10 HOMOs and 10 LUMOs). In contrast to the situation found for $Cp_2Ti(C{\equiv}CR)_2$, calculations suggest that there is significantly less mixing between the $\pi$-symmetry orbitals of the metallocycle and the Cp–M bonding orbitals. The HOMO is predominantly (91%) composed of metallacycle $\pi$ orbitals (Figure 4 (top)). The SHOMO ($12b_1$) is mostly Cp–M bonding with 20% localized on the metallacycle (Figure 4 (middle)). The third and fourth filled orbitals ($20a_1$ and $12b_2$) are $\sigma$ bonding between the Ti and the $\alpha$ carbons of the metallocycle, e.g. Figure 4 (bottom). The degree of mixing between metallacycle $\pi$ and $Cp_2Ti$ fragment orbitals is low enough that the MOs can be described by what type of bonding they represent in the complex (last column of Table IV).

## Discussion

It is remarkable how close our calculated structure for $Cp_2\overline{TiCH{=}CHCH{=}C}H$ is to the crystallographically determined tetraphenyl derivative. In general, ab initio calculations performed on metallocene complexes have predicted bond lengths between the metal and the Cp that are too long, unless electron correlation is included.[19] Indeed, it has been reported that the basis set superposition error (BSSE) compensates for the bond lengthening caused by this lack of correlation to lead some calculations to fortuitously predict correct geometries.[20] These problems, however, arise in complexes where the d orbitals are occupied. A 3d orbital has a highly contracted radial component; in fact, the radial distribution is quite similar to that of the 3s and 3p orbitals. Since the effect of correlation on core electrons is pronounced, one can easily suppose that electron correlation would be necessary to treat any system with occupied 3d orbitals in the valence region. Similarly, electron correlation is often necessary in systems where the large size of the ligand leads to repulsion that cannot be adequately treated without the inclusion of electron correlation.[21] Such effects are important, but since the calculations in this paper contain neither occupied 3d orbitals (except through partial occupation as the titanium orbitals stabilize what are essentially carbon orbitals) nor ligands of large size, they are unlikely to have much effect. Indeed, similarly successful results have been previously reported in titanium(IV) systems treated at a similar level of theory.[11,22]

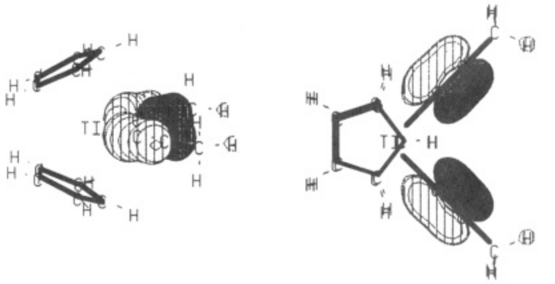

**Figure 5.** Molecular orbital plots[18] for the $21a_1$ orbital of $Cp_2Ti(C{\equiv}CMe)_2$. The view to the left is ca. along the $x$ axis, and the view to the right is along the $y$ axis.

Strong $\pi$ donation involving ligand orbitals and the metal-based LUMO (Figure 2) is commonly found in amide and alkoxide compounds of group 4 metallocenes.[23] Spectroscopic evidence suggests $\pi$ donation may be important in metallocene acetylide complexes as well.[24] However, we see only slight evidence for $\pi$ donation from the alkyne orbitals to the metal. The alkyne $\pi$ orbital that has the best overlap with the metal based LUMO is the $21a_1$, shown in Figure 5. The weakness of the interaction here is presumably due to the large energy difference between the $21a_1$ and the LUMO.

Another unexpected result is the significant amount of mixing between alkynyl $\pi$ and Cp orbitals. The top eight filled valence MOs are mixtures of alkynyl $\pi$ and Cp–M

---

(19) (a) Guest, M. F.; Hillier, I. H.; Vincent, M.; Rosi, M. *J. Chem. Soc., Chem. Commun.* **1986**, *438*. (b) Luthi, H. P.; Siegbahn, P. E. M.; Almolf, J. *J. Phys. Chem.* **1985**, *89*, 2156. (c) Luthi, H. P.; Siegbahn, P. E. M.; Almolf, J.; Faegri, K., Jr. Heiberg, A. *Chem. Phys. Lett.* **1984**, *111*, 1. (d) Almolf, J.; Faegri, K., Jr.; Schilling, B. E. R.; Luthi, J. P. *Chem. Phys. Lett.* **1984**, *106*, 266.

(20) Seijo, L.; Barandiaran, Z.; Klobukowski, M.; Huzinaga, S. *Chem. Phys. Lett.* **1985**, *117*, 151.

(21) Williamson, R. L.; Hall, M. B. *ACS Symp. Ser.* **1989**, *No. 394*, 17.

(22) (a) Koga, N.; Obara, S.; Morokuma, K. *J. Am. Chem. Soc.* **1984**, *106*, 4625. (b) Obara, S.; Koga, N.; Morokuma, K. *J. Organomet. Chem.* **1984**, *270*, C33. (c) Pietro, W. J.; Hehre, W. J. *J. Comp. Chem.* **1983**, *4*, 241. (d) Koga, N.; Morokuma, K. *Chem. Rev.* **1991**, *91*, 823.

(23) (a) Vann Bynum, R.; Hunter, W. E.; Rogers, R. D.; Atwood, J. L. *Inorg. Chem.* **1980**, *19*, 2368. (b) Huffman, J. C.; Moloy, K. G.; Marsella, J. A.; Caulton, K. G. *J. Am. Chem. Soc.* **1980**, *102*, 3009.

(24) Sebald, A.; Fritz, P.; Wrackmeyer, B. *Spectrochim. Acta* **1985**, *41A*, 1405.

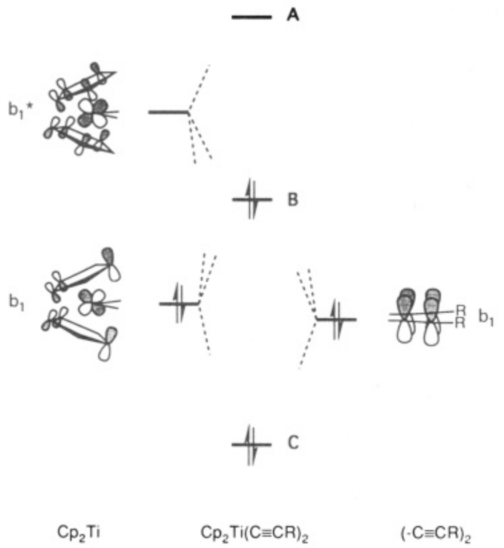

**Figure 6.** Filled–filled interaction scheme for $b_1$ symmetry $Cp_2Ti$ and bisacetylide fragments. A–C refer to orbital drawings shown in Figure 7.

bonding orbitals. The mixing is most likely the result of filled–filled interactions between Cp–M bonding and acetylide $\pi$ orbitals of appropriate symmetries. This type of interaction has been postulated for $CpFeL_2C{\equiv}CR$ (L = CO, $PR_3$; R = H, alkyl)[25] and recently verified by PES.[26,27] In the iron system the filled–filled interactions are between metal nonbonding orbitals and acetylide $\pi$ orbitals. For $Cp_2Ti(C{\equiv}CR)_2$ the top eight filled molecular orbitals contain *two* each of the four possible symmetries in $C_{2v}$ ($a_1$, $a_2$, $b_1$, $b_2$); see Table II. Each of the four Cp–M bonding orbitals in a bent metallocene fragment (i.e. $Cp_2Ti$) has a different symmetry, leading to a set of MOs containing one of each of the $C_{2v}$ symmetries.[9b,e,10] The two alkynyl $\pi$ systems combine to also give four orbitals with one of each of the $C_{2v}$ symmetries.[28] A filled–filled interaction for the titanocene acetylide system is illustrated for the $b_1$ symmetry orbitals in Figure 6. The plots shown for the three molecular orbitals formed by this interaction are shown in Figure 7. Three fragment orbitals are considered in this scheme; these are acetylide $\pi$ and Cp–M bonding and antibonding orbitals (see Figure 6). The lowest energy molecular orbital formed by the interaction ($13b_1$) is bonding between the metal and both the Cp and acetylide ligands. This MO is stabilized relative to all of the fragment orbitals. The middle energy orbital ($14b_1$) is destabilized with respect to the two filled fragment orbitals. This MO is bonding between the metal and the Cp ligands but antibonding between the metal and the acetylide ligands. At the chosen contour level for the plots in Figure 7 the metal orbitals are not observed. The highest energy orbital is all antibonding and is destabilized relative to all of the fragment MOs. Similar filled–filled interactions act to mix the $a_2$ and $b_2$ symmetry orbitals as well; see Table II. The top three filled MOs ($14b_1$, $7a_2$, $16b_2$) have a greater contribution from the $\beta$ carbon of the acetylide ligand than from the $\alpha$ carbon; see Table III. This polarization is due to the antibonding interaction between the metallocene fragment and the acetylide $\pi$ orbital in these MOs. A similar observation was made by Kostić and Fenske for $CpFeL_2C{\equiv}CH$.[25]

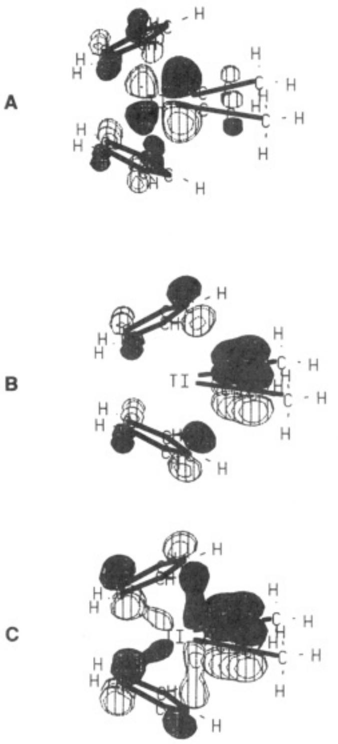

**Figure 7.** Molecular orbital plots[18] for MOs formed by filled-filled interaction shown in Figure 6. A–C refer to the labels shown in Figure 6 and are the $13b_1$, $14b_1$, and $15b_1$ MOs, respectively.

In contrast to the acetylide complexes, there is very little mixing between the $\pi$-symmetry orbitals of the metallacycle and the like symmetry Cp–Ti bonding orbitals. Two important differences between the structures of $Cp_2Ti(C{\equiv}CR)_2$ and $Cp_2\overline{TiCH{=}CHCH{=}C}H$ are the lengthening of the Ti–$C_\alpha$ bond (2.071 and 2.111 Å, respectively) and the decrease in the $C_\alpha$–Ti–$C_\alpha$ angle (93 and 81°, respectively). The $a_2$ symmetry metallacycle orbital is principally interacting with the $d_{xy}$, while the $b_1$ interacts with the $d_{yz}$.[28] The difference in overlap can be seen in the calculated overlap of the $C_\alpha$ $p_y$ orbitals with these d orbitals for the two structures. For $Cp_2Ti(C{\equiv}CH)_2$ the overlaps of the $C_\alpha$ $p_y$ orbitals with the $d_{xy}$ and $d_{yz}$ orbitals are 0.089 and 0.085, respectively. The same overlaps for $Cp_2\overline{TiCH{=}CHCH{=}C}H$ are 0.074 and 0.087. Considering the similarity of the overlaps, the decrease in mixing is observed for both the $a_2$ and $b_1$ symmetry orbitals of $Cp_2\overline{TiCH{=}CHCH{=}C}H$ relative to $Cp_2Ti(C{\equiv}CR)_2$ is surprising (see Tables II and IV). The reason for the decrease is that the degree of mixing also depends on the relative energies of the interacting orbitals. The metallocycle $\pi$ and $Cp_2Ti$ fragment orbitals of like symmetry are very far apart in energy. The $a_2$ symmetry orbitals are effectively pure metallacycle and CpTi-based MOs ($6a_2$ and

---

[25] Kostić, N. M.; Fenske, R. F. *Organometallics* **1982**, *1*, 974.

[26] Lichtenberger, D. L.; Renshaw, S. K. *Abstracts of Papers, 203rd ACS National Meeting of the American Chemical Society, San Francisco*, CA; American Chemical Society: Washington, DC, 1992; INORG 35.

[27] Photoelectron spectroscopy is the most direct way to examine the energies and compositions of MOs in molecular species. Unfortunately, these titanocene complexes are not amenable to PES. $Cp_2M(C{\equiv}CPh)_2$(M = Ti, Zr, Hf) and $Cp'_2Ti(C{\equiv}CC_4H_9)_2$ decompose to low-valent Ti species before their vaporization, precluding PES studies: Lichtenberger, D. L.; Renshaw, S. K. Unpublished results.

[28] The four combinations of the alkynyl $\pi$ system and their symmetry designations are given below. The darkened and open circles present $p_y$ orbitals.

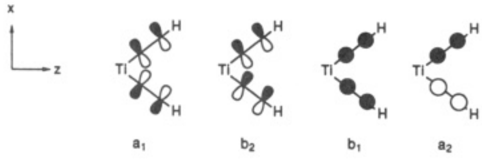

$5a_2$, respectively) and are spaced 3.9 eV apart. $CpFe(PH_3)_2(C{\equiv}CH)$ and $CpFe(PH_3)_2(N{\equiv}CH)^+$ show a similar relationship between the energies of the ligand $\pi$ orbitals and the degree of mixing brought about by filled–filled interactions.[25] The nitrile's $\pi$ level is at a much lower energy than that of the acetylide, leading to a negligible interaction between the nitrile $\pi$ system and the metal-based orbitals. The $b_1$ metallacycle $\pi$ orbital ($11b_1$, Table IV) is at much lower energy than the analogous bisacetylide orbital ($13b_1$, Table II). The degree of interaction between the metallacycle and $Cp_2Ti$ $b_1$ orbitals is low, but some mixing is observed ($12b_1$ and $11b_1$). This filled–filled interaction leads to polarization of the metallacycle $\pi$ system toward the $\beta$ carbon in the $12b_1$ orbital (Figure 4, middle), as observed for the acetylide complexes (vide supra).

From the data obtained for both $Cp_2\overline{TiCH{=}CHCH{=}CH}$ and $Cp_2Ti(C{\equiv}CR)_2$, an interesting comparison can be made. As the degree of s character in the bonding increases, the Ti–C bonds should become stronger. For $Cp_2TiMe_2$, $Cp_2\overline{TiCH{=}CHCH{=}CH}$ and $Cp_2Ti(C{\equiv}CH)_2$ the degree of s character in bonding increases, since the carbons $\sigma$-bound to titanium are $sp^3$, $sp^2$, and sp hybridized, respectively. The trend in bond strengths is clearly seen in the Ti–C bond lengths for these complexes, i.e. 2.152 (3),[29] 2.111, and 2.071 Å, respectively. Trends are also observed in orbital energies. In the dimethyl compound the HOMO and SHOMO orbitals are $Ti{-}CH_3$ $\sigma$ bonding.[10] For the metallacycle the HOMO and SHOMO are $\pi$ bonding orbitals and the third and fourth filled orbitals are the Ti–C $\sigma$-bonding set. In $Cp_2Ti(C{\equiv}CH)_2$ the $\sigma$-bonding set comes at very low energies; they are the ninth and tenth filled orbitals ($20a_1$ and $14b_2$). The increasing stability of the Ti–C $\sigma$-bonding orbitals is clearly seen in the calculated energies of these orbitals as well. The $\sigma$-bonding orbitals for $Cp_2TiMe_2$ are at −4.71 and −4.74 eV,[10] for $Cp_2\overline{TiCH{=}CHCH{=}CH}$ they are at −8.8 and −9.2 eV, and for $Cp_2Ti(C{\equiv}CH)_2$ the Ti–C $\sigma$-bonding orbitals are at −12.5 and −12.8 eV.

## Conclusion

Very little evidence is seen in our calculations for $\pi$ donation from filled acetylide orbitals to vacant metal-based orbitals, as proposed on the basis of crystallographic studies.[30] In addition very little mixing is observed between the ligand $\pi$ orbitals and the Cp–M bonding orbitals of ($Cp_2\overline{TiCH{=}CHCH{=}CH}$). The lack of mixing in both of these situations arises from poor energy matching of the interacting orbitals, since the degree of orbital overlap in both cases is similar to that observed for $Cp_2Ti(C{\equiv}CR)_2$.

Our study adds support to the postulate made by others[11] that substitution of chloride or hydride for Cp ligands may give an incorrect picture for bent metallocene complexes. While this simplification saves a great deal of time computationally, it may lead to an incorrect representation of the electronic structure. Hydride or chloride ligands would not have led to the same mixed states that were observed for $Cp_2Ti(C{\equiv}CR)_2$. It is important to note, however, that the type of filled–filled interaction observed here will probably only be important for hydrocarbyl ligands with filled $\pi$ orbitals, which lie at energies similar to those of the Cp–M bonding orbitals of like symmetry. A similar conclusion was drawn by Hehre for $Cp_2Ti{=}CH_2$.[11c]

The conclusion that can be drawn from the calculations reported here is that there is a significant amount of mixing between like symmetry $\pi$ orbitals of acetylide ligands and Cp–Ti bonding orbitals in $Cp_2Ti(C{\equiv}CR)_2$ complexes (R = H, $CH_3$). The reason for this mixing comes predominantly from good energy matches between the interacting fragment orbitals. Extended electronic networks such as these may be responsible for the observed third-order NLO properties of group 4 metallocene complexes. Substitution on the Cp or acetylide ligands will change the $\pi$-orbital energies, allowing us to "fine tune" the degree of delocalization, via mixing of "$Cp_2Ti$" and alkynyl $\pi$ orbitals. We are currently examining the NLO properties of other metallocene acetylide and vinylic complexes, related to those studied herein, to see if these properties are correlated with the degree mixing between metallocene and ligand $\pi$ orbitals.

## Experimental Section

The GAUSSIAN 86 computer program was used in this work.[31] Full geometry optimizations were performed at the STO-3G level[22c,32] within the restrictions of $C_{2v}$ symmetry and linear triple bonds. Double-$\zeta$, single-point calculations were performed at two different levels: the 3-21G level[33] and a more expanded basis with the 6-31G basis[34] on the ligands and the Rappe, Smedley, and Goddard d orbitals[35] in combination with a contracted Wachters' set[36] for the s and p on the titanium. Because of the consistency of the orbitals for identical molecules, we conclude that the results reported here are basis set independent. ZINDO calculations (Zerner's intermediate neglect of differential overlap program)[16] were run on a CAChe Worksystem[37] through a Macintosh environment. The three-dimensional orbital plots in this work were generated using the program PSI/77,[38] modified to accept coefficients and basis set information directly from GAUSIAN 86.[39] These MO plots shown throughout this paper are based on STO-3G calculations.

**Acknowledgment.** The authors thank Drs. Robert A. Pascal, Anthony K. Rappe, Michael C. Zerner, and Bruce E. Bursten for helpful discussions. This work was supported by the Dow Chemical Co., through their Cooperative Research Program, and the Air Force Office of Scientific Research (Grant AFOSR-90-0122).

**Supplementary Material Available:** Tables listing atom positions for the optimized geometries of $Cp_2Ti(C{\equiv}CR)_2$ (R = H, Me) and $Cp_2\overline{TiCH{=}CHCH{=}CH}$ (6 pages). Ordering information is given on any current masthead page.

OM920275Q

---

[29] The bond length for $Cp_2TiMe_2$ is not available, so the $Ti{-}CH_3$ bond length from $\eta^{10}$-(1,2-bis(3-(trimethylsilyl)cyclopentadienyl)tetramethylethane)$TiMe_2$ [$Me_4C_2(1\text{-}C_5H_3\text{-}3\text{-}TMS)_2TiMe_2$] is quoted in the text. See: Gutmann, S.; Burger, P.; Hund, H. H.; Hofmann, J.; Brintzinger, H. H. *J. Organomet. Chem.* **1989**, *369*, 343.

[30] Erker, G.; Fromberg, W.; Benn, R.; Mynott, R.; Angermund, K.; Kruger, C. *Organometallics* **1989**, *8*, 911.

[31] *Gaussian 86.* Frisch, M. J.; Binkley, J. S.; Schlegel, H. B.; Raghavachari, K.; Melius, C. F.; Martin, R. L.; Stewart, J. J. P.; Bobrowicz, F. W.; Rohling, C. M.; Kahn, L. R.; Defrees, D. J.; Seeger, R.; Whiteside, R. A.; Fox, D. J.; Fleuder, E. M.; Pople, J. A. Carnegie-Mellon Quantum Chemistry Publishing Unit: Pittsburgh, PA, 1984.

[32] Hehre, W. J.; Stewart, R. F.; Pople, J. A. *J. Chem. Phys.* **1969**, *51*, 2657.

[33] (a) Binkley, J. S.; Pople, J. A.; Hehre, W. J. *J. Am. Chem. Soc.* **1980**, *102*, 939. (b) Dobbs, K. D.; Hehre, W. J. *J. Comp. Chem.* **1987**, *8*, 861.

[34] Hehre, W. J.; Ditchfield, R.; Pople, J. A. *J. Chem. Phys.* **1972**, *56*, 2257.

[35] Rappe, A. K.; Smedley, T. A.; Goddard, W. A., III. *J. Phys. Chem.* **1981**, *85*, 2607.

[36] Wachters, A. J. H. *J. Chem. Phys.* **1970**, *52*, 1033.

[37] CAChe and the CAChe Worksystem are trademarks of Tektronics, Inc.

[38] Jorgensen, W. L. QCPE Program No. 344, 1977.

[39] Knight, E. T.; Jackson, J. E.; Kitchen, D. B. Unpublished results.